

# Comparison of Rolling Forces and Enlargement of Hot-rolled Strips Obtained from Experimental, Analytical and Simulation Models

Andre Rosiak<sup>a</sup>, Thomas Gomes dos Santos<sup>b\*</sup>, Diego Rafael Alba<sup>c</sup>, Alberto Moreira Guerreiro Brito<sup>d</sup>, Lirio Schaeffer<sup>e</sup>

<sup>a,b,c,d,e</sup>*Metal Forming Laboratory (LdTM), Federal University of Rio Grande do Sul (UFRGS),  
Av. Bento Gonçalves 9500, Porto Alegre, RS, Brazil*

<sup>a</sup>*Email: andre.rosiak@ufrgs.br,* <sup>b</sup>*Email: thomas.santos@ufrgs.br,* <sup>c</sup>*Email: diego.alba@ufrgs.br*

<sup>d</sup>*Email: brito@ufrgs.br,* <sup>e</sup>*Email: schaeffer@ufrgs.br*

## Abstract

During rolling processes, the strain on the thickness direction of a material inevitably results in dimensional changes in width and length. Knowledge of the behavior of strains and stresses acting during hot rolling process becomes indispensable, as it allows to estimate the resulting geometry and optimize process conditions. This study compares the deformation and the rolling forces obtained through experiments, analytical models and finite element simulation. To this end, SAE 1020 steel was hot processed in a duo rolling mill for reductions of 13%, 17% and 21% in height. Based on the performed experiments, a microstructural analysis was performed and a numerical model was proposed. Furthermore, these results were compared with different analytical models to determine the process characteristics. The numerical model obtained the better approximation among the approached models, with a discrepancy in the order of  $\pm 0.005\text{mm}$  in comparison with the measured values of the real deformation in width direction, what represents a relative error of 0.03%. Furthermore, the calculated force through simulation presented results closer to the ones measured experimentally presenting a good fit for the proposed model and hot rolling process. Finally, the processed microstructure migrated from elongated to equiaxed grains arising from the dynamic recrystallization mechanism. This study shows that numerical simulation had become an important tool to assess the development of rolling processes as they can predict the final geometry and forces with good correlation with real processing conditions.

**Keywords:** Hot rolling; Enlargement; Rolling Force; Numerical simulation; Analytical model.

---

\* Corresponding author.

**1. Introduction**

Rolling is a process of plastic deformation in which the material goes through rolls or cylinders causing a reduction in one of its dimensions, usually thickness, as shown in Figure 1. As a result of the reduction in thickness, and due to the law of volume constancy, a proportional increase occurs to other dimensions, i.e. width and length.

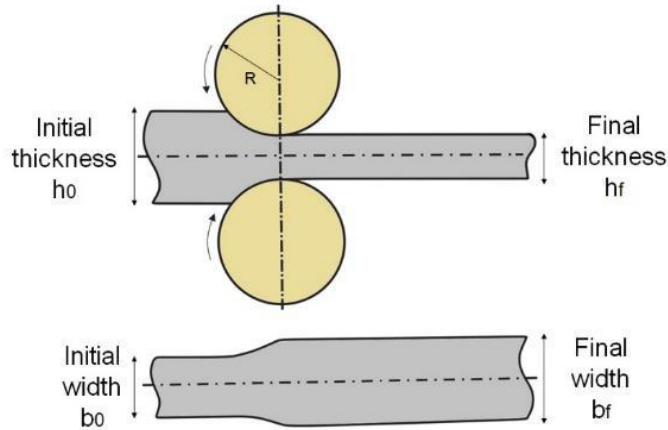


**Figure 1:** Schematic illustration of the geometrical changes during hot rolling [1].

The rolling process can be performed in hot or cold conditions, whereas cold rolling is mainly used in the production of sheets with thicknesses less than 1 mm [2]. Cold rolling imposes high dimensional accuracy on the laminated product, as well as giving it an increase in its mechanical strength due to hardening. Hot rolling is used in primary operations commonly applied to ingots as it enables greater reductions and lower rolling efforts. In the hot rolling process, due to the high temperature and deformation, there is the occurrence of metallurgical phenomena which influences the final properties of the laminated part as shown in Figure 2. Among these, it is possible to highlight the dynamic recrystallization, phenomenon resulting from the strains applied to the material combined with the high processing temperature [3-5]. According [6], recrystallization and the corresponding regeneration of the metallurgical structure are exclusive of hot rolling.

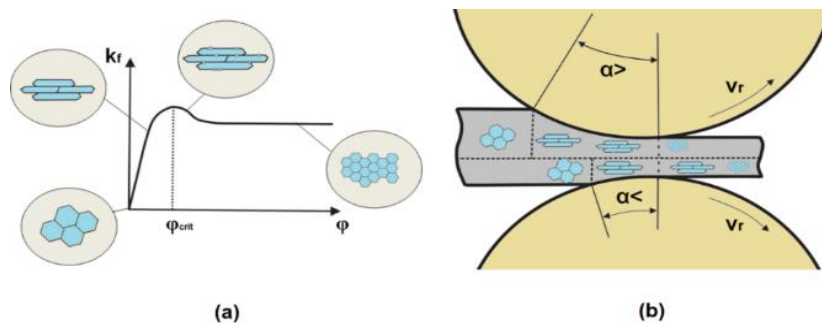


**Figure 2:** (a) Characteristic stress-strain curve hot formed materials for a determined temperature and strain rate. (b) Expected microstructural evolution after hot rolling process [6].

The need to understand the influential variables in the process for the correct definition of the mechanical properties allowing the direct application of laminates in final products was emphasized by [7]. With the application of hot rolling as a final process, it is extremely important to understand the strains of the rolled product and the stresses acting during rolling. This directly influences the finishing of the laminated product, and in addition productivity and processing efficiency. Regarding the strains and displacements, it is possible to emphasize the deformation in width direction, also known as enlargement. Usually, during the rolling process a greater elongation — deformation in length direction — of processed material is desired, since the widths are limited by the length of the lamination cylinders. Correctly predicting the enlargement in hot the rolling is difficult and the choice of methods that could accurately predict the material behavior during processing is extremely important. On this behalf, finite element analysis arises as a crucial tool to predict metal forming processes [8]. In the past, FEM has widely been applied to predict the metal flow in strips during cold and hot rolling processes [9]. Its application has been proved successful with regard to revealing most detailed aspects of metal flow characteristic in 2D and 3D rolling, either steady or non-steady-state [10-13]. The objective of this study is to compare the values of enlargement and rolling forces obtained in an analytical manner and by numerical simulation with the values measured during experiments. Divergences between the obtained results were evaluated and the method that best applies to the performed procedure was indicated.

## 2. Materials & Methods

This study was performed according to the following methodology.

### 2.1. Experimental procedure

In this study, the rolling of three SAE 1020 steel specimens was performed, with dimensions of 12.7 x 12.7 x 200 mm, being, respectively, height, width and length. The chemical composition of the material used is presented in Table 1.

**Table 1:** Chemical composition of SAE 1020 [14].

<b>%C</b>	<b>%Mn</b>	<b>%Si</b>	<b>%Cr</b>	<b>%Cu</b>	<b>%Ni</b>
0,18 – 0,23	0,3 – 0,6	0,1 – 0,2	0,15	0,2	0,15

Figure 3 shows the optical micrograph of the base material in the as received condition with 500x magnification. It is possible to verify that the microstructure consists in a matrix o elongated grains of pro-eutectoid ferrite (light colored). In addition, perlite colonies (dark-colored) are present, forming the typical microstructure of this steel class [15].

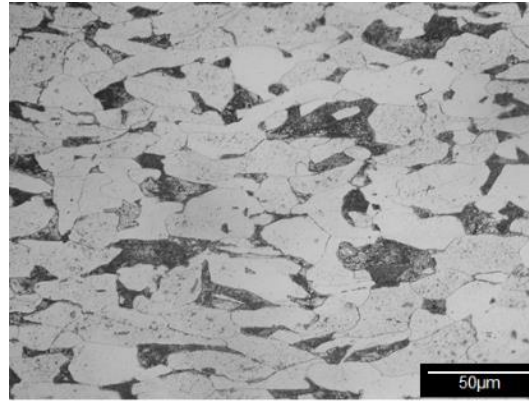


**Figure 3:** Optical micrograph of the SAE 1020 steel in the condition as received; Magnification: 500x; Etchant: Nital 3%.

For the experiments, the specimens were homogeneously heated in a muffle furnace to a temperature of approximately 1050°C and hold on this level for approximately 60 minutes. Due to thermal losses as a virtue of convection during the transport of the specimen to the rolling mill, a temperature of 1000 ° C was estimated for the specimens at the beginning of the process. After heating and transport, the specimens were rolled to reductions of 13%,17% and 21% in their height. The equipment used for the experiments was a “Duo” rolling mill and its characteristics are presented in Table 2.

**Table 2:** Hot-roller characteristics.

Length of cylinders' table	200	[mm]
Diameter of rolling cylinders	178,8	[mm]
Maximum gap between cylinders	16,8	[mm]
Peripheral velocity	252,8	[mm/s]
Cylinders' rotational speed	27	[rpm]

After rolling and cooling of the laminated material to room temperature, the dimensional measurements of the specimens were performed. The arithmetic mean of the height, width and length measurements were adopted, according to Equation 1.

$$M_d = \frac{n_1+n_2+n_3+\dots+n_x}{N} \quad (1)$$

Where:  $n_1, n_2, n_3$  to  $n_x$ = measured values;  $N$ = Number of measurements. Measurements were performed with the aid of a caliper with a resolution of 0.05 mm and the values were recorded for later comparison with the values of the analytical models and simulation. The rolling forces were measured with equipment developed by the LdTM/UFRGS (Metal Forming Laboratory – Federal University of Rio Grande do Sul) to acquire and measure the rolling force directly coupled to the rolling mill. The values were recorded for later comparison with the values of the rolling force obtained theoretically.

### 2.2. Analytical models

Firstly, the fundamental parameters of the rolling process were determined. For this, based on [16], the values of the deformation and strain in height, width and length were calculated. For the determination of the final rolling enlargement, several analytical models were used which are presented in Table 3.

**Table 3:** Analytical models to determine the enlargement after rolling [7].

Model	Equation
Siebel	$\Delta b = C_s \cdot l_d \cdot \frac{\Delta h}{h_0}$ (2)
Tafel & Sedlaczek	$\Delta b = \frac{0,435 \cdot b_0 \sqrt{b_0 \cdot r} \cdot \Delta h}{b^2 + h_0 \cdot h_1}$ (3)
Ekelund	$b_1^2 - b_0^2 = 8 \cdot m \cdot l_d \cdot \Delta h - 4 \cdot m \cdot (h_0 + h_1) \cdot l_d \cdot \ln \frac{b_1}{b_0}$ (4)
	$m = \frac{1,6 \cdot \mu \cdot l_d - 1,2 \cdot \Delta h}{h_0 + h_1}$ (4.1)
Köster	$\frac{\varphi_b}{\varphi_h} = -e \left( -C_{b\mu} \frac{b_0}{l_d} \right)$ (5)
	$C_{b\mu} = \frac{T_{ref}}{T_{lam}}$ (5.1)
Wusatowski	$\beta = \frac{b_1}{b_0} = \left( \frac{h_1}{h_0} \right)^{-w}$ (6)
	$-w = -10 \left( -1,269 \cdot \varepsilon W^{0,556} \cdot \frac{b_0}{h_0} \right)$ (6.1)
	$\varepsilon W = \frac{h_0}{2R}$ (6.2)

Where:  $\Delta b$ = Deformation in width;  $C_s$ = Correlation coefficient for Siebel model based on rolling temperature (for SAE 1020 steel at 1000°C,  $C_s=0,35$ );  $l_d$ = Contact arc;  $\Delta h$ = Deformation in height;  $h_0$ = Initial height;  $r$ = Rolling cylinders radius;  $b, b_0$ = Initial width;  $h_1$ = Final height;  $b_1$ = Final width;  $\mu$ = Friction coefficient;  $\varphi_b$ = true strain in width direction;  $\varphi_h$ = true strain in height direction;  $T_{ref}$ = Reference temperature = 1000;  $T_{lam}$ = Rolling temperature in Kelvin. The rolling force was calculated following the methodology presented in [7]. The following equations were considered for this calculation. To determine the yield stress, Equation 7 was used where  $\vartheta$  it represents the temperature in degrees Celsius [17].

$$k_{fm} = 10 \cdot (0,14 - 0,01 \cdot \vartheta) \cdot (1,4 + \%C + \%Mn + 0,3 \cdot \%Cr) \quad (7)$$

Equation 8.1 was used to determine the term  $C_\mu$ , considering  $\vartheta$  as the rolling temperature in Kelvin and the term  $h_m$  is the mean value between the initial and final height of the specimen. Posteriorly, this term was inserted in Equation 8.

$$k_1 = \exp \left( C_\mu \cdot \frac{l_d}{h_m} \right) \quad (8)$$

$$C_{\mu} = \frac{T_{lam}^{-996}}{T_{lam}} \quad (8.1)$$

After the solution of Equation 8, the calculated value was introduced in Equation 9 to determine the resistance to deformation.

$$k_w = k_{fm} \cdot k_1 \quad (9)$$

The result of Equation 9 was used to determine the rolling force according to Equation 10, being  $A_d$  the contact area between the cylinder and the rolled part.

$$F = A_d \cdot k_w \quad (10)$$

With the solution of Equation 10 it was possible to compare the values of rolling forces obtained experimentally.

### 2.3. Numerical model

**Table 4:** Simulation input parameters.

Billet material	AISI 1020	
Initial temperature	1000	[°C]
Element type	Hexagonal	
Mesh size	0,74	[mm]
Rolling cylinders' initial temperature	25	[°C]
Ambient temperature	25	[°C]
Cylinders' velocity	27	[rpm]
HTC Convection	10	[W/(m <sup>2</sup> .K)]
HTC Conduction	3500	[W/(m <sup>2</sup> .K)]
Emissivity	0,88	[-]
Orowan friction model	$\mu=0.3;$ $m=0.5$	[-]

The finite element module of the software *Simufact Forming 15.0* provided by *MSC Software Corporation* was used for numerical simulation. A 3D model was proposed where the cylinders were defined as rigid elements with heat conduction. The considered blank material, from the software library, was SAE 1020 steel with an elastoplastic behavior. The input parameters for the numerical model are presented in Table 4. In order to reduce the simulation time, two symmetry planes were considered as shown in Figure 4.

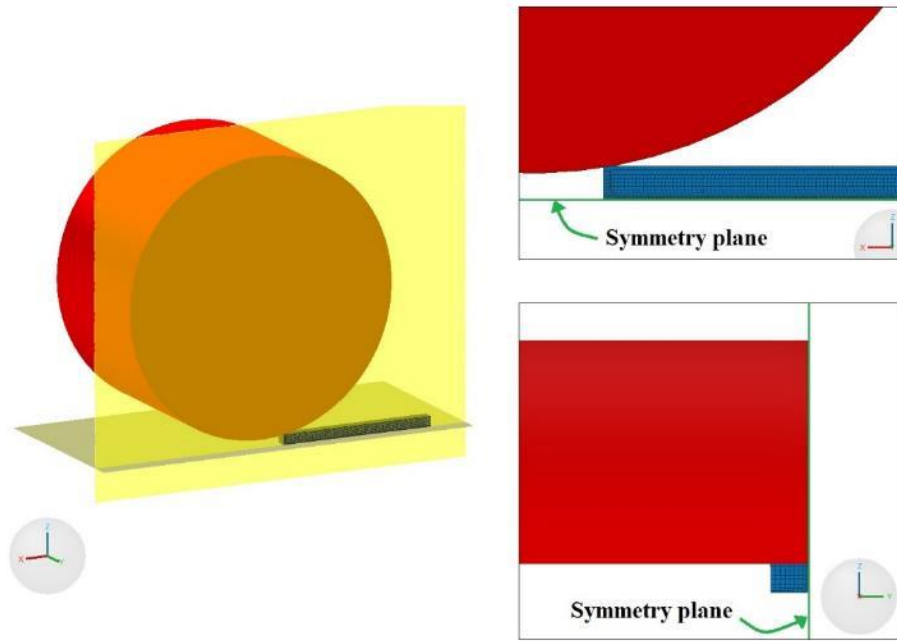


**Figure 4:** Finite element model for the hot rolling process.

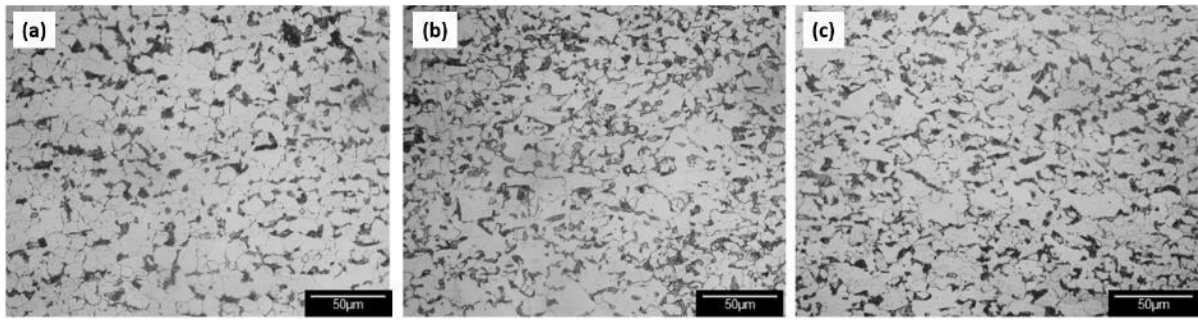
### 3. Results & Discussions

Figure 5 shows the tested specimens according to the previously described methodology. According to the law of volume constancy, larger reductions in height result in larger dimensions in the length and width are expected.



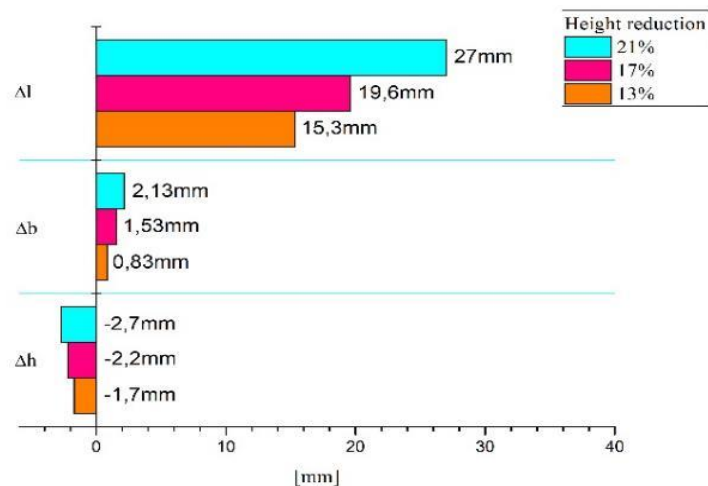
**Figure 5:** Final geometry of specimens after hot rolling process. Height reductions of (a) 21%, (b) 17% and (c) 13%.

Figure 6 shows the optical micrographs of the samples with 21 (a), 17 (b) and 13% (c) of reduction in thickness. Analyzing the microstructures after the hot rolling process, it is evident that the dynamic recrystallization process took place for all the different deformation levels imposed [18;19]. In the grain contours of the distorted structure in the received condition (Figure 3), new refined and equiaxial grains were nucleated.



**Figure 6:** Optical micrograph of the SAE 1020 steel after the hot rolling process; (a) 13%, (b) 17% and (c) 21% of reduction in height; Magnification: 500x; Etchant: Nital 3%.

When compared to each other, the final microstructures in which a higher degree of deformation has been established presented a more refined grain structure. This occurs because new formed grains are prevented from growing due to the imposed deformation [4;20]. The sample with 13% thickness reduction, however, experienced more pronounced grain growth after recrystallization. During rolling, the new dynamically recrystallized grains stop growing and remain small, since the thermodynamic potential is being created inside the new grains due to the continuous plastic deformation. The increase in free energy caused by the introduction of new grain boundaries is compensated by the decrease in free energy due to the elimination of crystalline defects (dislocations). In this way, as the potential difference through the boundaries of the new grains decreases, they stop growing. On the other hand, in samples subjected to less deformation, the grains stopped growing only when they found their neighbors who are also growing. Thus, grain refinement is not effective. From the measurements of the rolled specimens, the values of the change in dimensions of height, width and length were determined. The measured values are presented in Figure 7.



**Figure 7:** Absolute deformation of the hot rolled specimens.

Analyzing Figure 7 it is possible to observe that the values of the change in the dimensions corresponded to the predicted, since for the experiment with 21% of reduction in height resulted in superior change in the values of



width and length, fact attributed to the law of volume constancy. Figure 8 shows the results for effective plastic strain for the simulation model for all the applied reductions. Furthermore, it is possible to extract the results for plastic strain in ZZ direction (height) and compare these results with the experimental data. Thus, based on the results of reduction on height presented in Figure 7, and in hands of Equation 11, the true strain in height direction is calculated. The results of the true strain in height are presented on Table 5. Comparing the calculated values with the simulations model is possible to conclude that the model presented a reasonable fit for these results. The discrepancy when the comparison between experimental and simulated plastic strain results is made can be attributed to the stiffness of the rolling mill and cylinders. Whereas the simulation considers the rolling cylinders as complete rigid materials, the cylinders of the rolling mill could elastic deform during the process. Furthermore, is not possible to assure that the stiffness of the equipment is high enough to prevent the cylinders axis to translate during process.

$$\varphi_h = \ln \left( \frac{h_0}{h_1} \right) \tag{11}$$

**Table 5:** Plastic strain in height direction.

Nominal reduction	Plastic strain in height direction - experimental	Plastic strain in height direction - simulation
13%	-0.1437	-0.1267
17%	-0.1902	-0.2128
21%	-0.2128	-0.2651

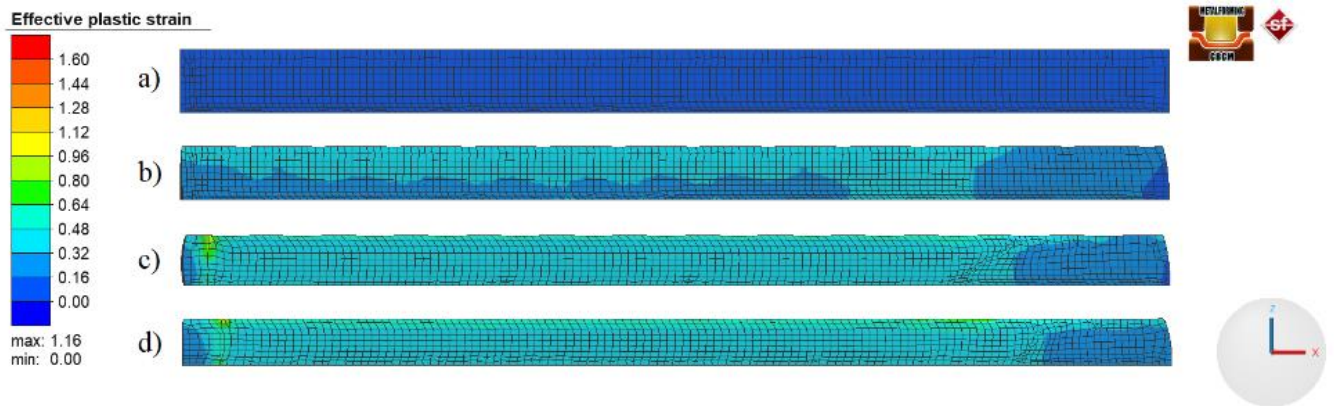


**Figure 8:** FEM results for effective plastic strain at different reductions. (a) before processing; (b) 13%; (c) 17% and (d) 21%.

The rolling forces obtained experimentally were plotted against time, as shown in Figure 9, and the values of the respective forces were considered by the calculated averages.

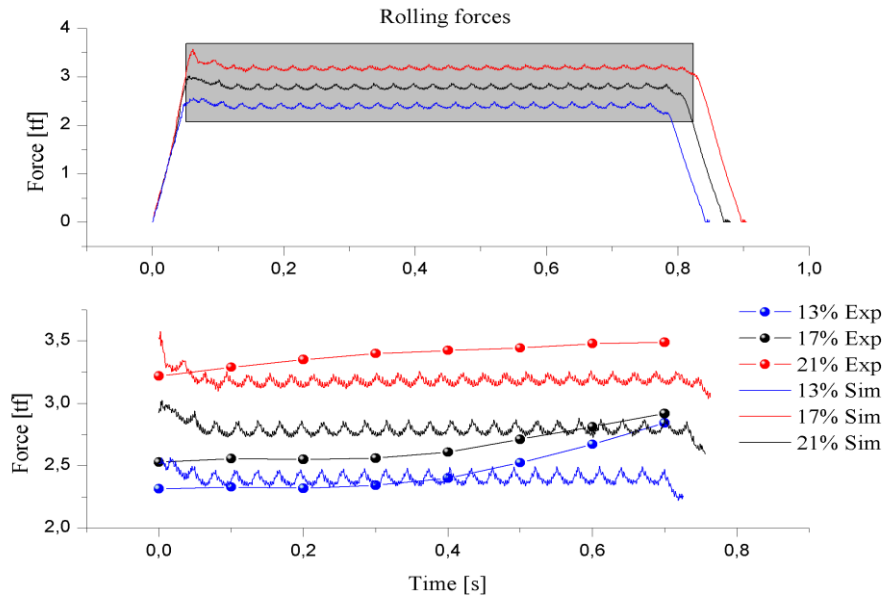


**Figure 9:** Hot rolling force values obtained by experiments and numerical simulation, (a) simulation model (b) comparison between experiments and simulation.

Analyzing Figure 9, it is observed that at the beginning of the rolling process, the required force is lower when compared to the final moments. In addition, the rolling force increases with the rolling time, an event possibly influenced by the temperature of the specimens. Since the material loses its initial temperature (1000°C) to the rollers due to conduction, its mechanical resistance increases, making it necessary a greater force to deform. After the data treatment of force and enlargement from the experiments, it was possible to compare it with the values calculated analytically. These results are presented in Figure 10 and Figure 11.

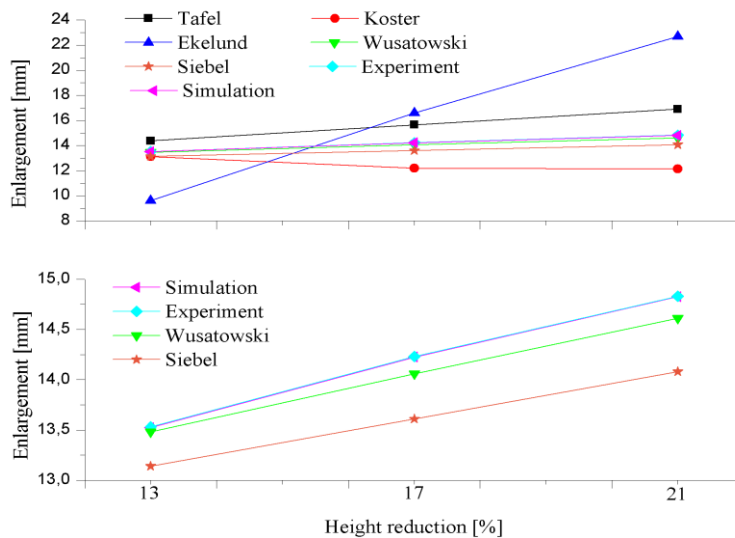


**Figure 10:** (a) Comparison between experimental, analytical and simulation values for deformation in width direction. (b) detail of the models that presented better fit with experimental values.

When comparing the experimentally obtained enlargement values with various analytical methods, Wusatowski method was the model with better accuracy when compared to the experimental results, having a maximum relative error of 1.5% in the value of enlargement to 21% reduction. The numerical model used for this work obtained the best approximation among the models considered here, obtaining a difference of the order of  $\pm 0.005\text{mm}$  having and a relative error of 0.03% when compared with the value of the experimentally measured enlargement.

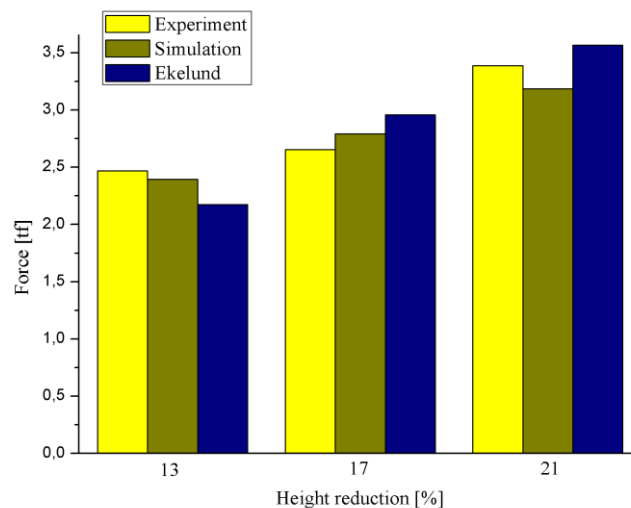


**Figure 11:** Comparison between experimental, simulated and Ekelund model values for hot rolling forces.

It is observed that the values of the rolling force corresponded to the expected, since as the percentage of reduction increases the values of the rolling forces should be higher. This occurs as a result of the need for greater energy to deform the material. Once again, the FEM model was shown to be highly accurate to estimate rolling force. The maximum relative error was -5% and occurred in the model for a reduction in height of 21%. Nevertheless, the values of the rolling forces obtained analytically according to Ekelund, when compared to the experimental values, presented a good accuracy with a maximum error of 8%. It is important to highlight that the approximation found between numerical simulation and experiments is due to the enormous similarity between numerical model and physical model. For other experiments all the boundary conditions must be precisely evaluated in order to obtain accurate results when compared to the studied physical model. The model presented on this study is for a steel strip with ratio  $b/h = 1$ . This must be taken into account since the deformations in bodies with a ratio  $b/h \neq 1$  could result in certain discrepancies between the theoretical models and simulations. These discrepancies can be attributed to the contact zone with the rolling cylinder, which influences the deformation directions. The friction on the interface between strip and cylinders leads, preferentially, to a deformation in the longitudinal direction for bodies with the ratio  $b/h > 1$  and deformation in the transverse direction for bodies with a ratio  $b/h < 1$ .

#### 4. Conclusions

Different analytical models were applied and compared with experiments and numerical simulation to determine the deformation in width direction and forming forces in hot rolling experiments with AISI 1020 steel specimens for reductions of 13%, 17% and 21%. The following conclusions can be drawn from this study.

- Deformation results presented values were as expected. Larger reductions in height resulted in higher values of deformation in height and width. This is attributed to the law of volume constancy and plastic behavior of the material.
- Rolling force values increased over time, an event that can be attributed to a reduction in the temperature of the specimens during the process. The cooling of the specimens is caused by convective, radiative and conductive thermal losses, where the conductive loss between the specimen, the lamination table and the rolling cylinders has the greatest influence for the performed experiment. During the experiments, the cylinders and the lamination table were at room temperature, and with the cooling of the material, its deformability was reduced, resulting in the need for greater energy for deformation due to the increase of its mechanical resistance.
- The numerical model used for this work obtained the best approximation among the models considered to estimate enlargement. This assertion is also valid when it was desired to estimate the rolling force during the process. For enlargement, a difference in the order of  $\pm 0.005\text{mm}$  was measured having a relative error of 0.03% when compared with the values experimentally measured. Regarding rolling force, the maximum relative error of the simulated model was -5%.
- Among the analytical models, it is noted that the Wusatowski method was the model with better accuracy to estimate enlargement when compared to the experimental results.
- The values of the rolling forces obtained analytically according to Ekelund method, when compared to the experimental values, were shown to be highly accurate. Therefore, it is advisable to use this model to determine the rolling force in similar experiments with specimens' ratio of  $b/h=1$ .

#### Acknowledgements

The authors would like to thank CAPES and CNPq for the sponsored scholarships.

#### References

- [1]. E. BRESCIANI FILHO, I.B. SILVA, G.F. BATALHA, et al. *Conformação Plástica dos Metais*, 6 ed.. São Paulo: EPUSP, 2011.
- [2]. J. RODRIGUES, P. MARTINS. *Tecnologia mecânica: Tecnologia da Deformação Plástica*, Vol. I, 1 ed.. Lisboa: Escolar, 2005.
- [3]. C.M. SELLARS, J.A. WHITEMAN. "Recrystallization and grain growth in hot rolling". *Metal Science*, v. 13, n. 3-4, pp. 187 – 194, 1979.
- [4]. K. HUANG, R.E. LOGÉ. "A review of dynamic recrystallization phenomena in metallic materials". *Materials and Design*, v. 111, pp. 548 – 574, 2016.

- [5]. F.H. SAMUEL, S. YUE, S.S. JONAS, et al, “Effect of dynamic recrystallization on microstructural evolution during strip rolling”. *ISIJ International*, v. 30, n. 3, pp. 216 – 225, 1990.
- [6]. J. RODRIGUES, P. MARTINS. *Tecnologia mecânica: Tecnologia da Deformação Plástica*, Vol. 2, 1 ed.. Lisboa: Escolar, 2005.
- [7]. N.C. SILVA. “Influência da laminação de encruamento sobre a planicidade e propriedades mecânicas de tiras de aço laminadas a quente”. Masters Thesis, UFOP, Ouro Preto, MG, Brazil, 2007.
- [8]. M.S. GADALA, J. WANG. “Simulation of metal forming processes with finite element methods”. *International Journal for Numerical Methods in Engineering*, v. 44, pp. 1397 – 1428, 1999.
- [9]. S. KOBAYASHI, S. OH, T. ALTAN. *Metal Forming and the Finite-Element Method*, 1 ed., New York: Oxford University Press, 1989.
- [10]. Y.J. HUW, J.G. LENARD. “A finite element study of flat rolling”. *Journal of Engineering Materials Technology*, v.110, n. 1, pp. 23 – 27, 1988.
- [11]. U.S. DIXIT, P.M. DIXIT. “Finite element analysis of flat rolling with inclusion of anisotropy”. *International Journal of Mechanical Science*, v. 39, n. 11, pp. 1237 – 1255, 1997.
- [12]. S.X. ZHOU. “An integrated model for hot rolling of steel strips”. *Journal of Materials Processing Technology*, v. 134, pp. 338 – 351, 2003.
- [13]. R.R. DEMA, A.N. SHAPOVALOV, V.V ALONTSEV, et al. “Computer simulation and research of the hot rolling process in DEFORM-3D”. *Materials Today: Proceedings*, Article in press.
- [14]. HANDBOOK COMMITTEE, *Metals Handbook Vol 14: Forming and Forging*, ASM International, 1989.
- [15]. HANDBOOK COMMITTEE, *Metals Handbook Vol. 9: Metallography and Microstructures*, ASM International, 1998.
- [16]. L. SCHAEFFER. *Conformação mecânica*, 3. ed., Porto Alegre: Imprensa Livre, 2009.
- [17]. S. EKELUND, Z. WUSATOWSKI. *Fundamentals in Rolling*, Oxford: Pergamon Press, 1969.
- [18]. Z. YANUSHKEVCH, A. BELYAKOV, R. KAIBYSHEV. “Microstructural evolution of a 304-type austenitic stainless steel during rolling at temperatures of 773-1273 K”. *Acta Materialia*, v. 82, pp. 244 – 254, 2015.
- [19]. V. BEDEKAR, P. PAUSKAR, R. SHIVPURI, et al. “Microstructure and texture evolution in AISI 1050 steel by flow forming”. *Procedia Engineering*, v. 81, pp. 2355 – 2360, 2014.
- [20]. T. SAKAI, A. BELYAKOV, R. KAIBYSHEV, H. MIURA, et al. “Dynamic and post dynamic recrystallization under hot, cold and severe plastic deformation conditions”. *Progress in Material Science*, v. 60, pp. 130 – 207, 2014.